

NACA RM L51H22



# RESEARCH MEMORANDUM

AERODYNAMIC CHARACTERISTICS AT TRANSONIC SPEEDS OF A

60° DELTA WING EQUIPPED WITH A CONSTANT-CHORD

FLAP-TYPE CONTROL WITH AND WITHOUT

AN UNSHIELDED HORN BALANCE

TRANSONIC-BUMP METHOD

By Harleth G. Wiley and Leon Zontek

Langley Aeronautical Laboratory  
Langley Field, Va.

CLASSIFIED DOCUMENT

This material contains information affecting the National Defense of the United States within the meaning of the espionage laws, Title 18, U.S.C., Secs. 793 and 794, the transmission or revelation of which in any manner to unauthorized person is prohibited by law.

FOR REFERENCE

NOT TO BE TAKEN FROM THIS ROOM

CLASSIFICATION CANCELLED

Auth: (by) NACA R7 2668 Date 9/10/47

By: DMDA 9424/54

## NATIONAL ADVISORY COMMITTEE FOR AERONAUTICS

WASHINGTON  
September 16, 1952

UNCLASSIFIED



UNCLASSIFIED

## NATIONAL ADVISORY COMMITTEE FOR AERONAUTICS

## RESEARCH MEMORANDUM

AERODYNAMIC CHARACTERISTICS AT TRANSONIC SPEEDS OF A  
60° DELTA WING EQUIPPED WITH A CONSTANT-CHORD  
FLAP-TYPE CONTROL WITH AND WITHOUT  
AN UNSHIELDED HORN BALANCE  
TRANSONIC-BUMP METHOD

By Harleth G. Wiley and Leon Zontek

## SUMMARY

An investigation to determine the control hinge moments and effectiveness at transonic speeds of a delta wing equipped with a constant-chord flap-type control with and without an unshielded triangular horn balance was made in the Langley high-speed 7- by 10-foot tunnel by means of the transonic-bump method. The wing was a semispan model with 60° of sweepback at the leading edge, an aspect ratio of 2.31, a taper ratio of 0, and an NACA 65-006 airfoil section parallel to the free air stream. The Mach number range investigated varied from 0.6 to 1.18; the mean Reynolds numbers varied from 1,100,000 to 1,400,000.

The data indicated that the horn-balance control was consistently more effective in changing lift at all Mach numbers than was the plain control but there was no appreciable difference in pitching-moment effectiveness.

Use of the triangular horn balance materially reduced the variation of hinge-moment coefficients with control deflection at all Mach numbers investigated and produced large positive values of  $C_{h\alpha}$  at subsonic speeds tending toward zero at supersonic speeds.

## INTRODUCTION

As part of an integrated program of transonic research carried on by the National Advisory Committee for Aeronautics, a semispan model of

CONFIDENTIAL

UNCLASSIFIED

a delta wing with  $60^\circ$  of sweepback at the leading edge, with an NACA 65-006 airfoil section, and with various control-surface configurations is being investigated by the transonic-bump method in the Langley high-speed 7- by 10-foot tunnel.

The results of an investigation of the model of a  $60^\circ$  delta wing with a triangular control having a skewed hinge axis and an overhang balance are given in reference 1. Presented in this paper are the results of an investigation of the model of the delta wing equipped with a constant-chord plain control, and with the control fitted with a large unshielded triangular horn balance. The purpose of the investigation was to determine and compare the control hinge moments and control-effectiveness parameters of the two configurations.

#### COEFFICIENTS AND SYMBOLS

$C_L$	lift coefficient $\left( \frac{\text{Twice lift of semispan model}}{qS} \right)$
$C_m$	pitching-moment coefficient referred to $0.25\bar{c}$ $\left( \frac{\text{Twice pitching moment of semispan model}}{qS\bar{c}} \right)$
$C_h$	control hinge-moment coefficient about hinge axis $\left( \frac{\text{Hinge moment}}{2M_1q} \right)$
$q$	effective dynamic pressure over span of model, pounds per square foot $\left( \frac{1}{2} \rho V^2 \right)$
$S$	twice wing area of semispan model (0.144 sq ft)
$b$	twice span of semispan model (0.578 ft)
$\bar{c}$	mean aerodynamic chord of wing $\left( \frac{2}{S} \int_0^{b/2} c^2 dy, 0.333 \text{ ft} \right)$
$y$	spanwise distance from plane of symmetry, feet
$c$	local wing chord, feet
$M_1$	area moment of control surface rearward of hinge axis, measured about hinge axis (0.00144 ft <sup>3</sup> )

$\rho$	mass density of air; slugs per cubic foot
$V$	average free-stream air velocity, feet per second
$M$	effective Mach number over span of model
$M_a$	average chordwise Mach number
$M_l$	local Mach number
$R$	Reynolds number of wing based on $\bar{c}$
$\alpha$	angle of attack, degrees
$\delta$	control deflection relative to wing-chord plane, measured perpendicular to control hinge axis (positive when trailing edge is down), degrees

$$C_{L\delta} = \left( \frac{\partial C_L}{\partial \delta} \right)_{\alpha}$$

$$C_{m\delta} = \left( \frac{\partial C_m}{\partial \delta} \right)_{\alpha}$$

$$C_{h\delta} = \left( \frac{\partial C_h}{\partial \delta} \right)_{\alpha}$$

$$C_{h\alpha} = \left( \frac{\partial C_h}{\partial \alpha} \right)_{\delta}$$

$$C_{L\alpha} = \left( \frac{\partial C_L}{\partial \alpha} \right)_{\delta}$$

The subscript  $\alpha$  indicates that the angle of attack was held constant at  $\alpha = 0^\circ$ .

The subscript  $\delta$  indicates that the control deflection was held constant at  $\delta = 0^\circ$ .

#### MODEL AND APPARATUS

Separate wing models were used for each control configuration. The semispan wings had  $60^\circ$  of sweepback at the leading edge,  $0^\circ$  sweep at the trailing edge, a taper ratio of 0, an aspect ratio of 2.31, and an NACA 65-006 airfoil section parallel to the free air stream. A sketch

of the models as mounted on the transonic bump is presented in figure 1. The wings were made of a bismuth and tin alloy bonded to a tapered steel core. Wing contours were generated by straight-line elements from the tip to the airfoil section at the root.

Both controls were similar rearward of the hinge line in that they had a constant chord equal to 20 percent of the root chord of the wing. The area rearward of the hinge line was 36 percent of the total wing area. The unshielded horn balance, triangular in shape, was mounted at the tip and the area was 41 percent of the control area rearward of the hinge line (fig. 1). Both controls had two support hinges: one about 1/3 span outboard on the wing and the other concealed in the housing of the bump.

The models were mounted on an electrical strain-gage balance which was enclosed within a chamber in the bump. The balance chamber was sealed except for a small rectangular clearance hole in the turn table through which an extension of the wing core passed. This hole was covered by a curved wing-root end plate, attached directly to the wing spar (fig. 1) and mounted approximately 1/16 inch above, and parallel to, the surface of the bump.

The wing lift, pitching moments, and control hinge moments were indicated by a calibrated electrical potentiometer.

#### TESTS

The tests were made in the Langley high-speed 7- by 10-foot tunnel utilizing an adaption of the NACA wing-flow technique for obtaining transonic speeds. The technique used involves placing the model in the high-velocity flow field generated over the curved surface of a bump as described in reference 2.

Typical contours of the local Mach number distribution over the test area of the bump with the model removed are shown in figure 2. The contours indicate that there was a Mach number variation of about 0.04 over the wing semispan at low Mach numbers and about 0.05 at the higher Mach numbers. The maximum chordwise Mach number variation was about 0.03. No attempt has been made to evaluate the effects of these chordwise and spanwise Mach number variations. The long dashed lines near the root of the wing indicate a local Mach number approximately 5 percent below the maximum value and represent the estimated thickness of the bump boundary layer. The effective test Mach number was

obtained from contour charts similar to those presented in figure 2 by using the relationship

$$M = \frac{2c}{\pi} \int_0^{b/2} cM_a dy$$

The variation of mean Reynolds number with Mach number is presented in figure 3 and varied from about 1,100,000 to about 1,400,000. The boundaries on the figure are an indication of the possible range in Reynolds number caused by variations in test conditions.

Force and moment data were obtained through a Mach number range of 0.6 to 1.18, an angle-of-attack range of  $-2^\circ$  to  $8^\circ$ , and a control-deflection range of  $-10^\circ$  to  $10^\circ$  for the plain control and  $-10^\circ$  to  $7^\circ$  for the horn-balance control.

#### CORRECTIONS

The lift and pitching moments represent data for the complete wing with controls mounted on both semispans. Aerodynamic effects on the wing of the attached end plate are unknown and consequently cannot be taken into account. The effects of the plate on lift, pitching moment, and control hinge moment are believed to be negligible. The controls and the wing proper, when statically loaded to anticipated air-load limits, were found to have negligible deflection in torsion and bending; therefore, no corrections for flexibility were applied.

#### RESULTS

The variations of lift, pitching-moment, and hinge-moment coefficients with control deflections for the angle-of-attack range at Mach numbers of 0.6, 1.00, and 1.18 for the plain control are presented in figures 4 to 6. Similar data for the balanced control are presented in figures 7 to 9. Figures 10 and 11 present the variation of lift, pitching-moment, and hinge-moment coefficients with control deflections at zero angle of attack through the Mach number range for the plain and balanced controls, respectively.

The variation of hinge-moment coefficient  $C_h$  at zero control deflection with angle of attack at each Mach number investigated is presented for both controls in figure 12, and a similar chart of lift coefficient  $C_L$  is presented in figure 13.

Hinge-moment and control-effectiveness parameters are presented in figures 14 and 15 and were taken from figures 4 to 13 over a range of angle of attack or control deflection of  $\pm 2^\circ$ .

Although the models employed symmetrical airfoil sections, asymmetry of data is apparent in figures 4 to 11. This asymmetry can be attributed to small inaccuracies in construction and to slight errors in setting angle of attack and control deflections during the tests.

## DISCUSSION

### Longitudinal Characteristics

Examination of figure 14 indicates that the horn-balance control was 40 to 80 percent more effective in producing changes in lift throughout the Mach number range than was the plain control, as might be expected because of the increased control area. Although both controls exhibited loss in lift effectiveness above  $M = 0.95$ , there was no appreciable difference in pitching-moment effectiveness for the two controls. The low value of pitching-moment effectiveness of the balanced control, which occurs in spite of the increase in lift effectiveness, is probably caused by a simultaneous forward movement of the center of pressure. The variations of lift and pitching moment with control deflection were more linear for the balanced control than for the plain control.

### Hinge-Moment Characteristics

The plain control exhibited negative values of  $C_{h_\alpha}$  throughout the Mach number range, as seen in figures 12 and 15. Addition of the triangular horn balance resulted in positive values of  $C_{h_\alpha}$  at subsonic speeds and approximately zero  $C_{h_\alpha}$  at supersonic speeds.

Examination of the hinge-moment parameter  $C_{h_\delta}$  for the plain control (fig. 14) reveals a negative increase with Mach number up to  $M = 0.97$  with a sharp reversal and consequent decrease in the transonic speed range. Use of the horn balance on the control materially reduced the hinge moments at all speeds and obtained aerodynamic balance at Mach numbers less than  $M = 0.8$ .

The large positive values of  $C_{h\alpha}$  of the horn control can be explained by consideration of the location of the center of lift. The design of the horn was dictated by the requirement that  $C_{h\alpha}$  be zero at all Mach numbers. An elliptical spanwise loading was assumed as predicted in reference 3 with the center of lift at the center of wing area or at  $0.50\bar{c}$ . Reference 4 shows, however, that the center of lift of a delta wing is nearer  $0.40\bar{c}$  at a Mach number of 0.6, indicating a general forward shift in local section centers of lift and explaining the overbalance with angle of attack at low Mach numbers. The center of lift then moves rearward with increase in Mach number until it approaches the theoretical position of  $0.50\bar{c}$  at and above sonic velocities with the consequent reduction in overbalance and the subsequent attainment of virtually complete aerodynamic balance with angle of attack at supersonic speeds.

The rearward shift in center of lift with increase in Mach number is also the reason for the high negative increase in  $C_{h\delta}$  above a Mach number of 0.8 as presented in figure 14. At Mach numbers less than 0.8, the aerodynamic load and center of lift of the horn were such as to balance the hinge moment of the control rearward of the hinge line. Increase in Mach number progressively shifted the local center of lift of the horn and control rearward, thus promoting a large negative increase in  $C_{h\delta}$  for the control surface.

#### Comparison with Other Delta-Wing Control Investigations

The plain control tested and described in this paper is generally similar to the constant-chord controls tested on other delta wings described in references 4 to 6. The physical characteristics and control parameters of the plain control of this paper and of the reference papers are presented in figure 16.

Examination of hinge-moment parameters  $C_{h\delta}$  for the four controls shows fair qualitative agreement in that  $C_{h\delta}$  increases with Mach number up to sonic speeds with a general tendency to decrease above  $M = 1.0$ .

The greatest discrepancy in trends in the comparisons of the characteristics of the delta wings and plain controls of this paper and the reference papers appears in the lift-effectiveness parameters  $C_{L\delta}$ . Data obtained by the transonic-bump technique of this paper and by the rocket-powered model of reference 6 are in good agreement and the same

general trend of decrease in  $C_{L\delta}$  with Mach number is exhibited in reference 4. The data of reference 5 show a slight increase in  $C_{L\delta}$  with Mach number in the subsonic range.

Curves of  $C_{L\alpha}$  against Mach number show the same qualitative trend of increasing values with increase in Mach number up to  $M = 1.0$  with a decrease beginning near a Mach number of unity.

#### CONCLUDING REMARKS

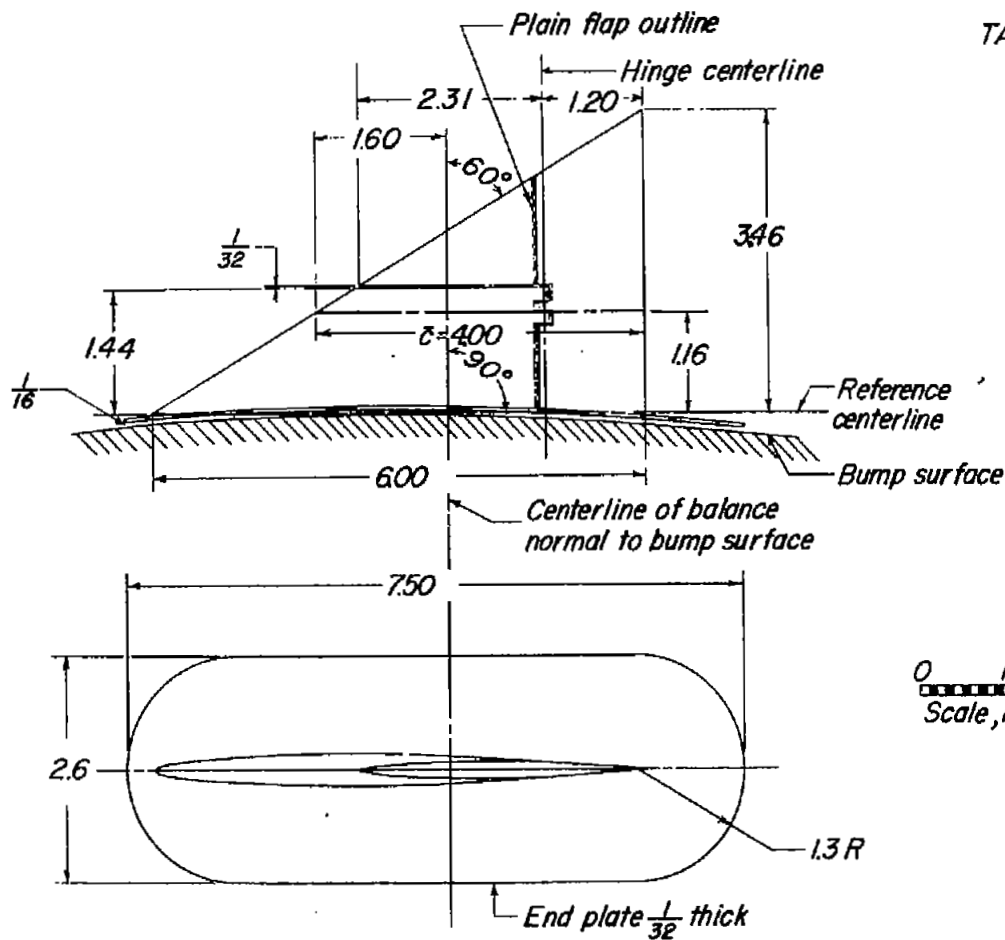
The results of an investigation on a  $60^\circ$  delta-wing model equipped with a constant-chord control with and without unshielded horn balance showed that the horn-balance control was more effective in producing a change in lift throughout the transonic Mach number range than was the plain control. Differences in pitching moment for the plain and horn-balance controls were negligible.

Application of the horn balance to the control overbalanced the control to give high positive values of the hinge-moment coefficient with angle of attack  $C_{h\alpha}$  in the subsonic speed range and essentially zero hinge moments with angle of attack above a Mach number of 1.0. Use of the balance materially reduced the values of  $C_{h\delta}$  at all speeds, actually obtaining aerodynamic balance at Mach numbers less than 0.8.

Langley Aeronautical Laboratory  
National Advisory Committee for Aeronautics  
Langley Field, Va.

## REFERENCES

1. Wiley, Harleth G.: Aerodynamic Characteristics at Transonic Speeds of a  $60^\circ$  Delta Wing Equipped with a Triangular Plan-Form Control Having a Skewed Hinge Axis and an Overhang Balance. Transonic-Bump Method. NACA RM L50L01, 1951.
2. Schneiter, Leslie E., and Ziff, Howard L.: Preliminary Investigation of Spoiler Lateral Control on a  $42^\circ$  Sweptback Wing at Transonic Speeds. NACA RM L7F19, 1947.
3. Jones, Robert T.: Properties of Low-Aspect-Ratio Pointed Wings at Speeds below and above the Speed of Sound. NACA Rep. 835, 1946. (Formerly NACA TN 1032.)
4. Rathert, George A., Jr., Rolls, L. Stewart, and Hanson, Carl M.: The Transonic Characteristics of a Low-Aspect-Ratio Triangular Wing with a Constant-Chord Flap As Determined by Wing-Flow Tests, Including Correlation with Large-Scale Tests. NACA RM A50E10, 1950.
5. Stephenson, Jack D., and Ameudo, Arthur R.: Tests of a Triangular Wing of Aspect Ratio 2 in the Ames 12-Foot Pressure Wind Tunnel. II - The Effectiveness and Hinge Moments of a Constant-Chord Plain Flap. NACA RM A8E03, 1948.
6. Mitcham, Grady L., Stevens, Joseph E., and Norris, Harry P.: Aerodynamic Characteristics and Flying Qualities of a Tailless Triangular-Wing Airplane Configuration As Obtained from Flights of Rocket-Propelled Models at Transonic and Low Supersonic Speeds. NACA RM L9L07, 1950.



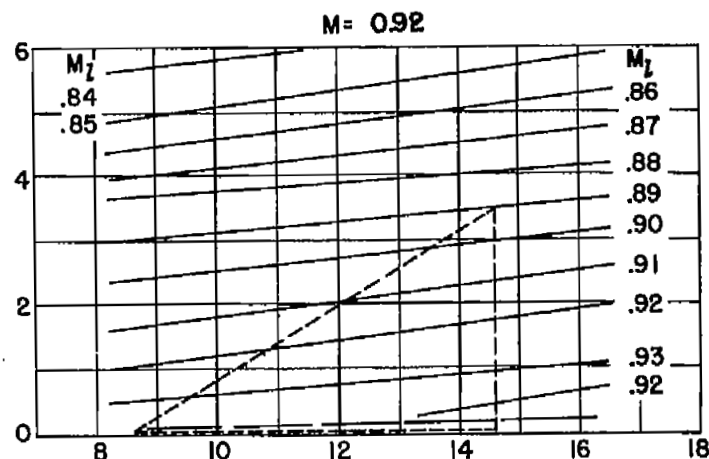
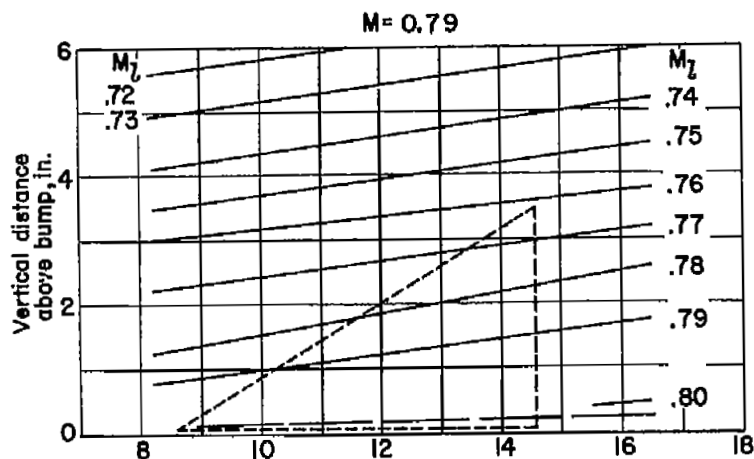
**TABULATED WING DATA**

Area (twice semispan)	0.144 sq ft
Mean aerodynamic chord	0.333 ft
Aspect ratio	2.31
Airfoil section parallel to free airstream	NACA65-006

0 1 2  
Scale, inches



Figure 1.- General arrangements of 60° swept delta-wing models, aspect ratio 2.31, NACA 65-006 airfoil having a 0.20-constant-chord flap-type control with and without an unshielded triangular horn balance.



----- Nominal boundary-layer thickness

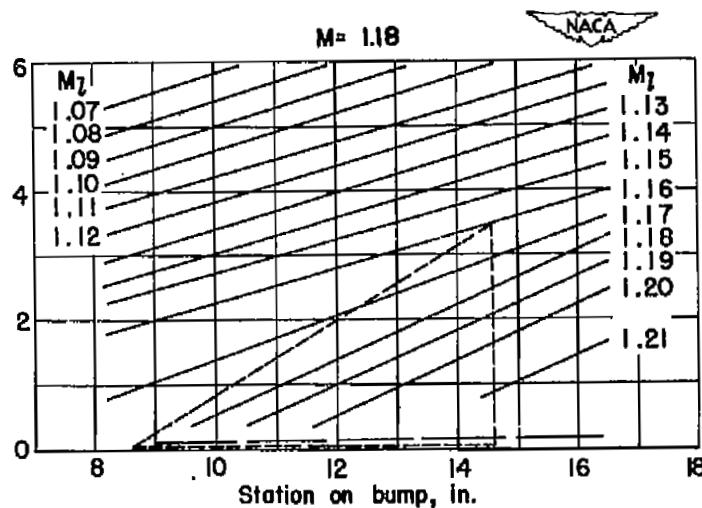
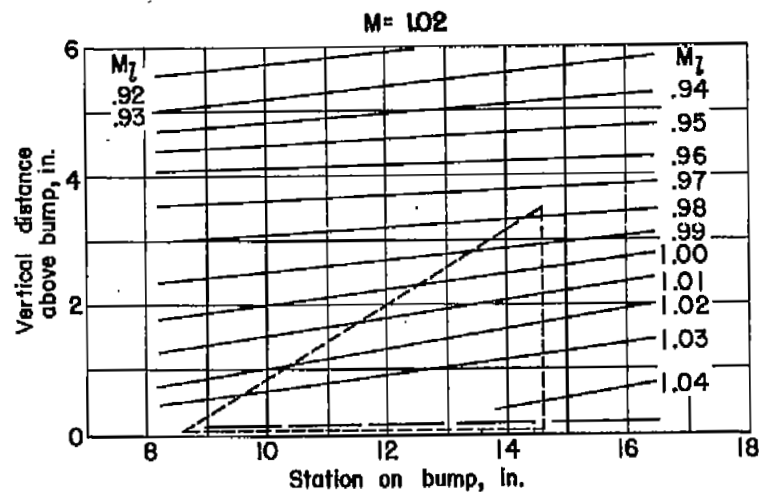


Figure 2.- Typical Mach number contours over transonic bump in region of model location.

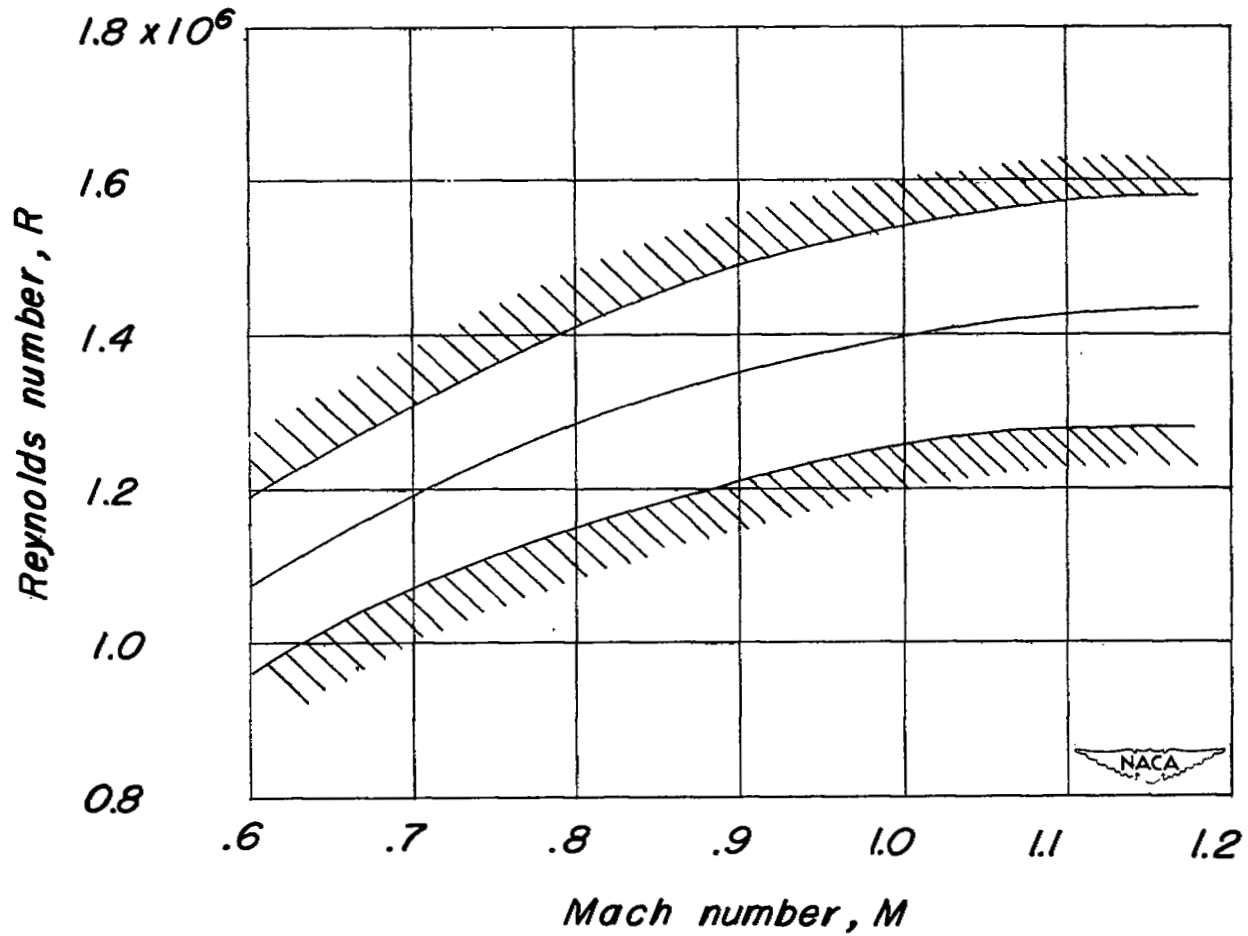


Figure 3.- Variation of test Reynolds number with Mach number for a  $60^\circ$  delta wing tested on the transonic bump.

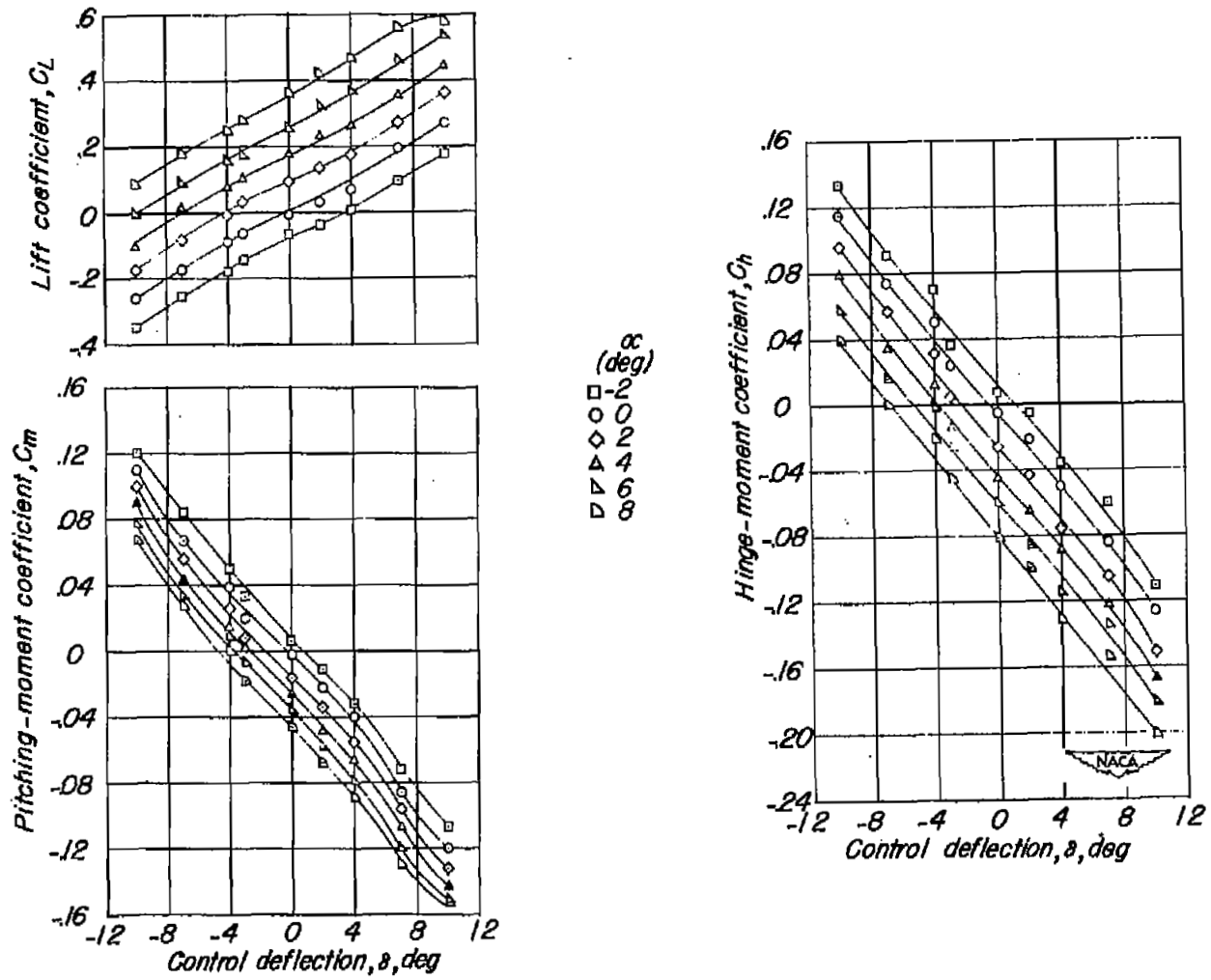
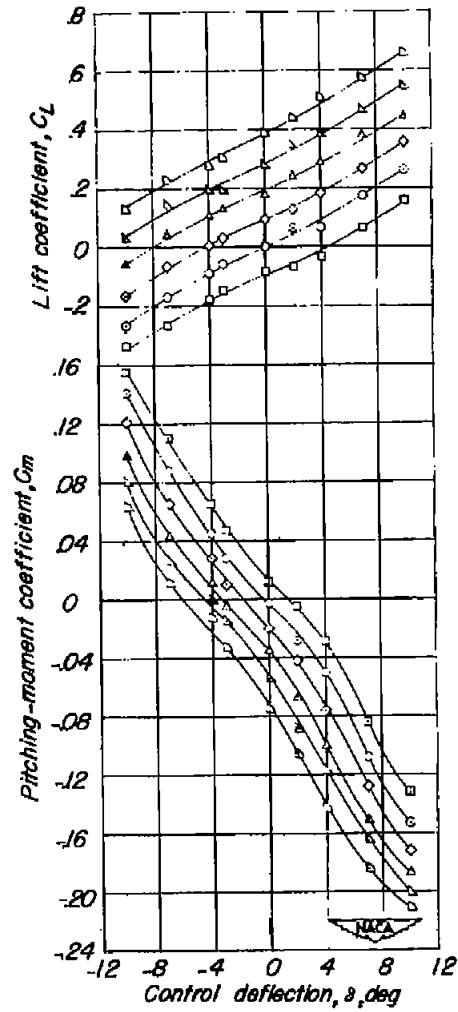


Figure 4.- Variation of aerodynamic characteristics with control deflection at various angles of attack for a  $60^\circ$  delta wing having a 0.20-constant-chord flap-type control.  $M = 0.60$ .



$\alpha$   
(deg)  
8  
6  
4  
2  
0

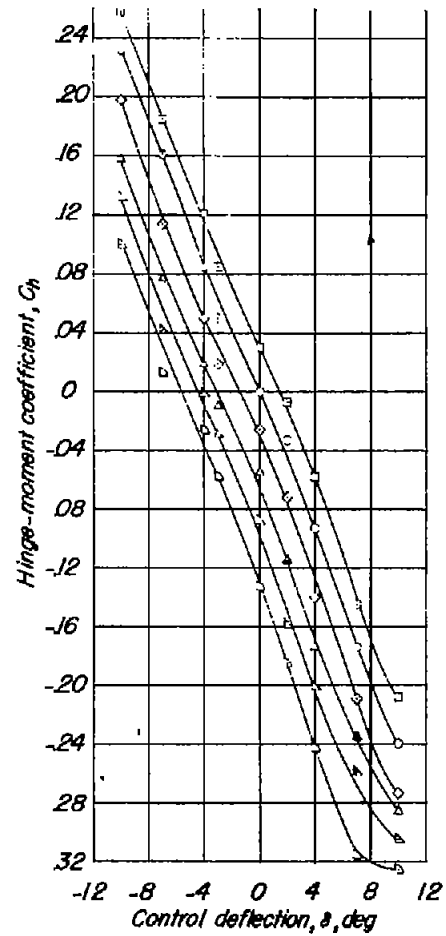


Figure 5.- Variation of aerodynamic characteristics with control deflection at various angles of attack for a  $60^\circ$  delta wing having a 0.20-constant-chord flap-type control.  $M = 1.00$ .

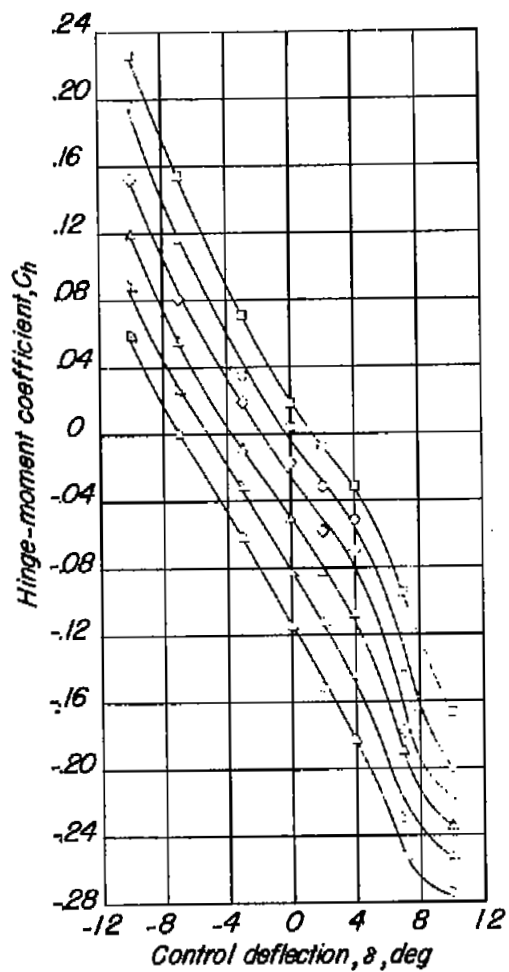
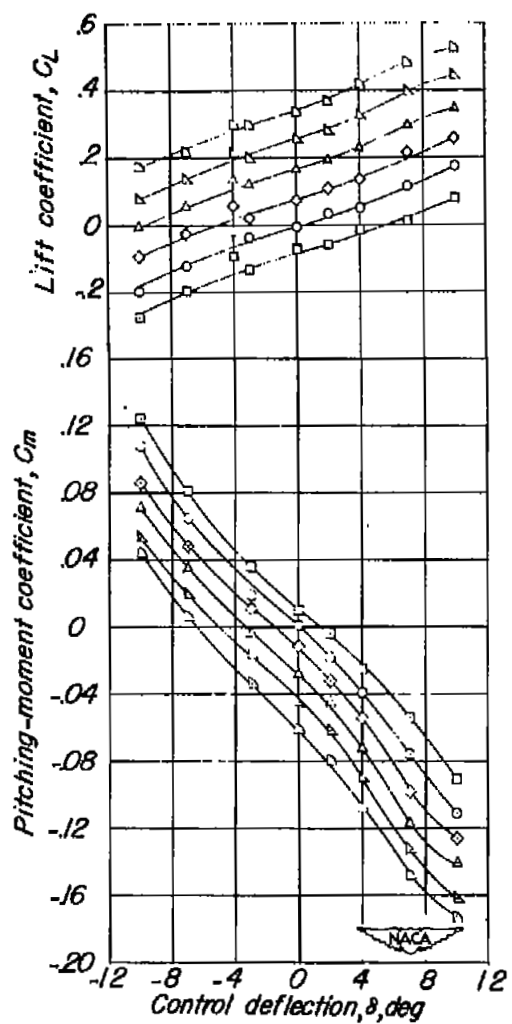


Figure 6.- Variation of aerodynamic characteristics with control deflection at various angles of attack for a 60° delta wing having a 0.20-constant-chord flap-type control.  $M = 1.18$ .

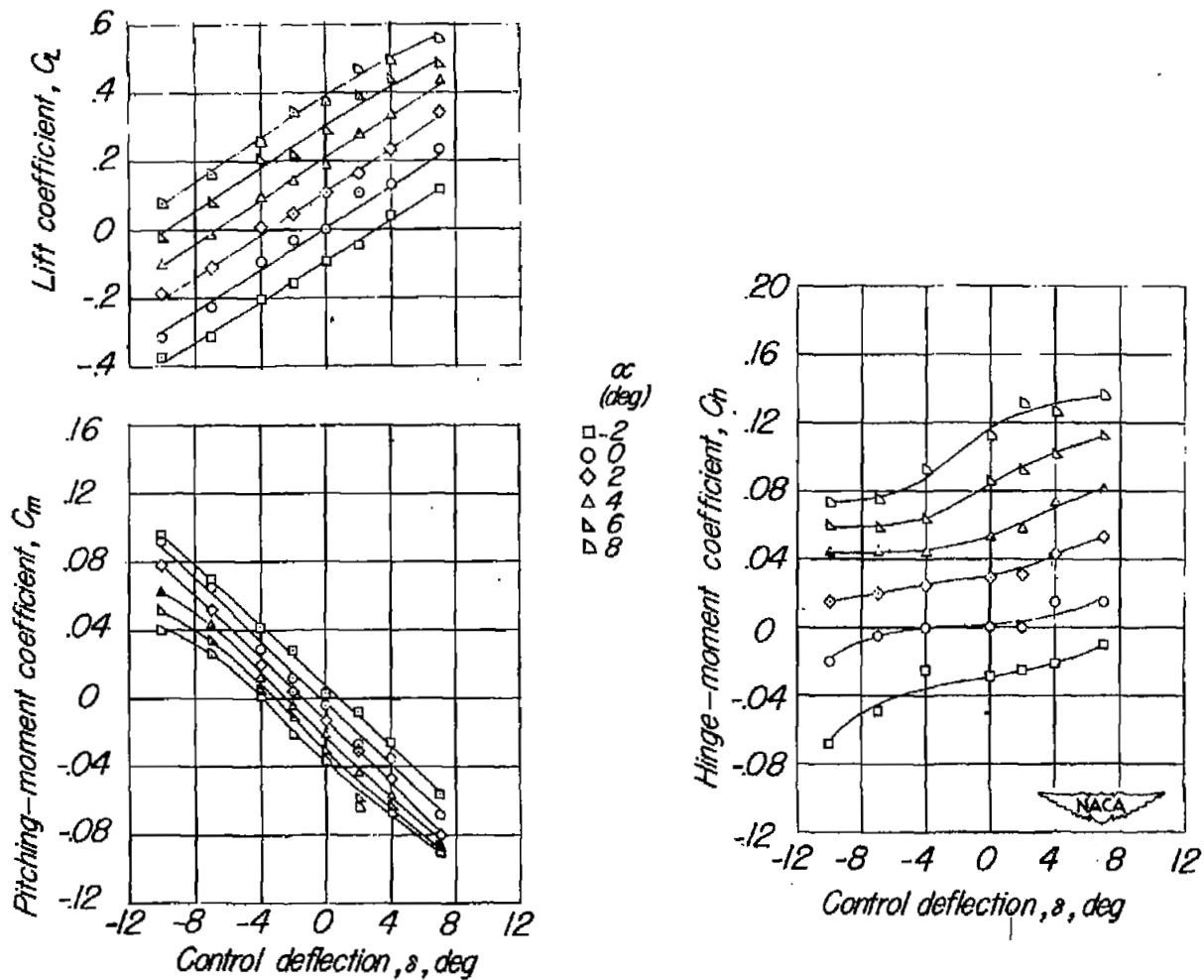


Figure 7.- Variation of aerodynamic characteristics with control deflection at various angles of attack for a  $60^\circ$  delta wing having a 0.20-constant-chord flap-type control with an unshielded triangular horn balance.  $M = 0.60$ .

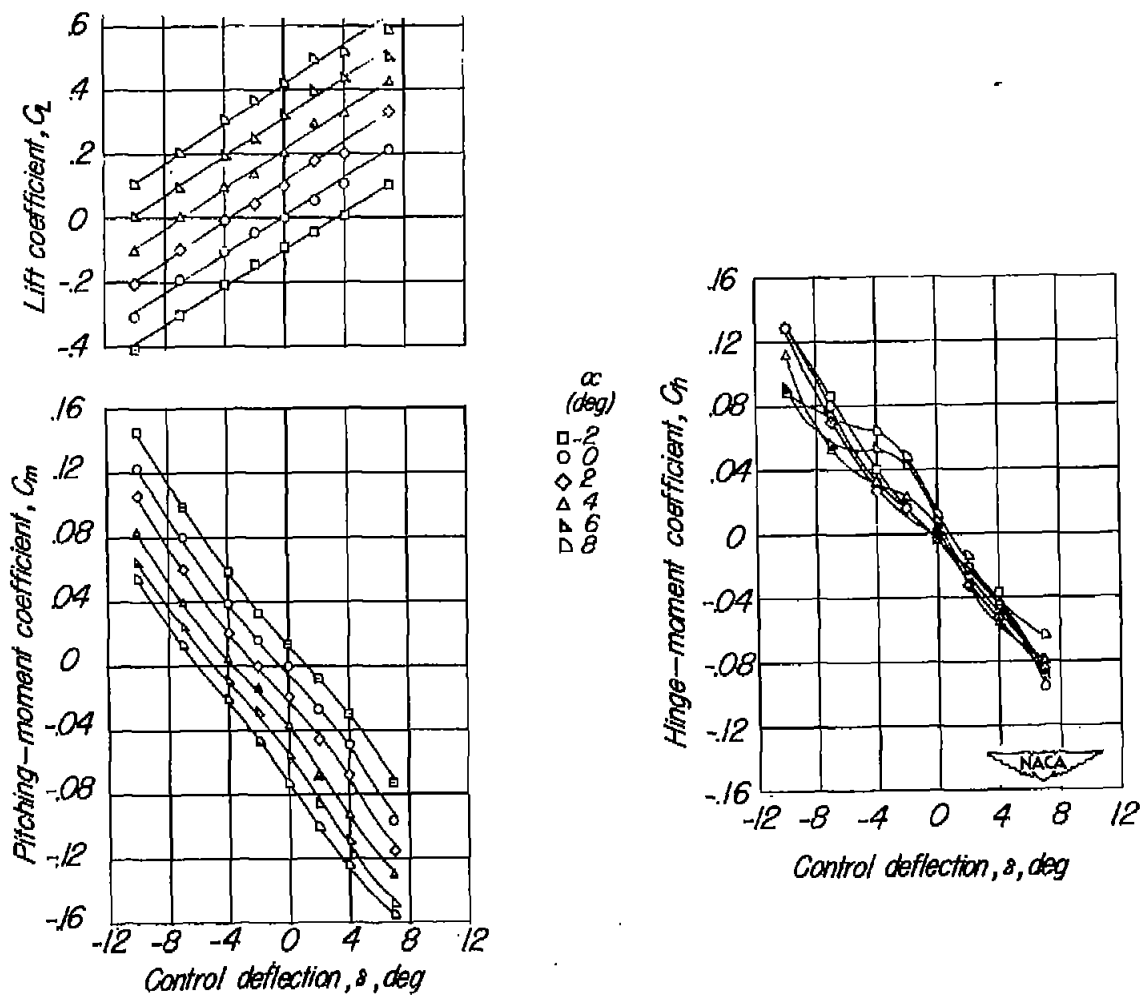
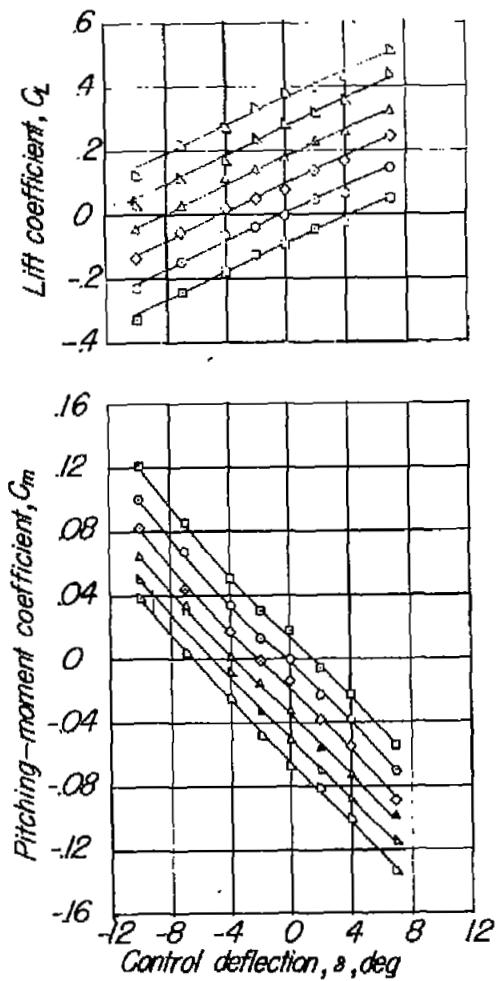


Figure 8.- Variation of aerodynamic characteristics with control deflection at various angles of attack for a  $60^\circ$  delta wing having a 0.20-constant-chord flap-type control with an unshielded triangular horn balance.  
 $M = 1.00$ .



$\alpha$   
(deg)

- 2
- 4
- ◇ 6
- △ 8
- ▽ 10
- 12

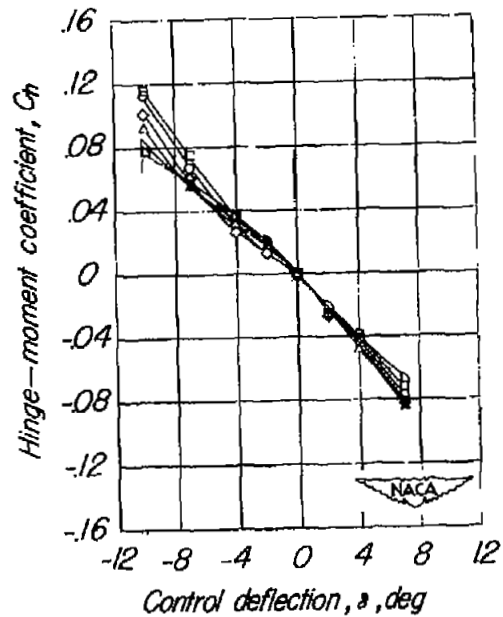


Figure 9.- Variation of aerodynamic characteristics with control deflection at various angles of attack for a  $60^\circ$  delta wing having a 0.20-constant-chord flap-type control with an unshielded triangular horn balance.  
 $M = 1.18$ .

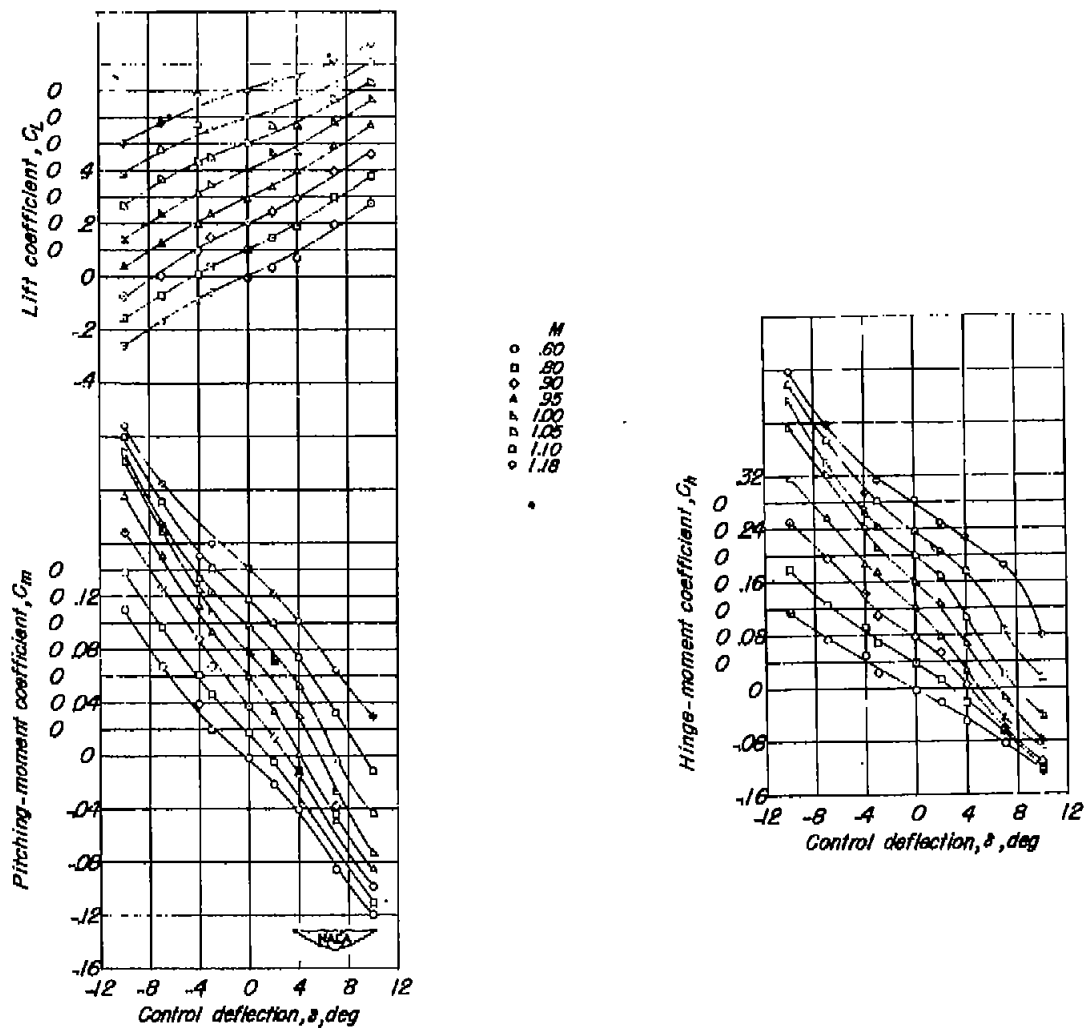


Figure 10.- Variation of aerodynamic characteristics with control deflection at various Mach numbers for a  $60^\circ$  delta wing having a 0.20-constant-chord flap-type control.  $\alpha = 0^\circ$ .

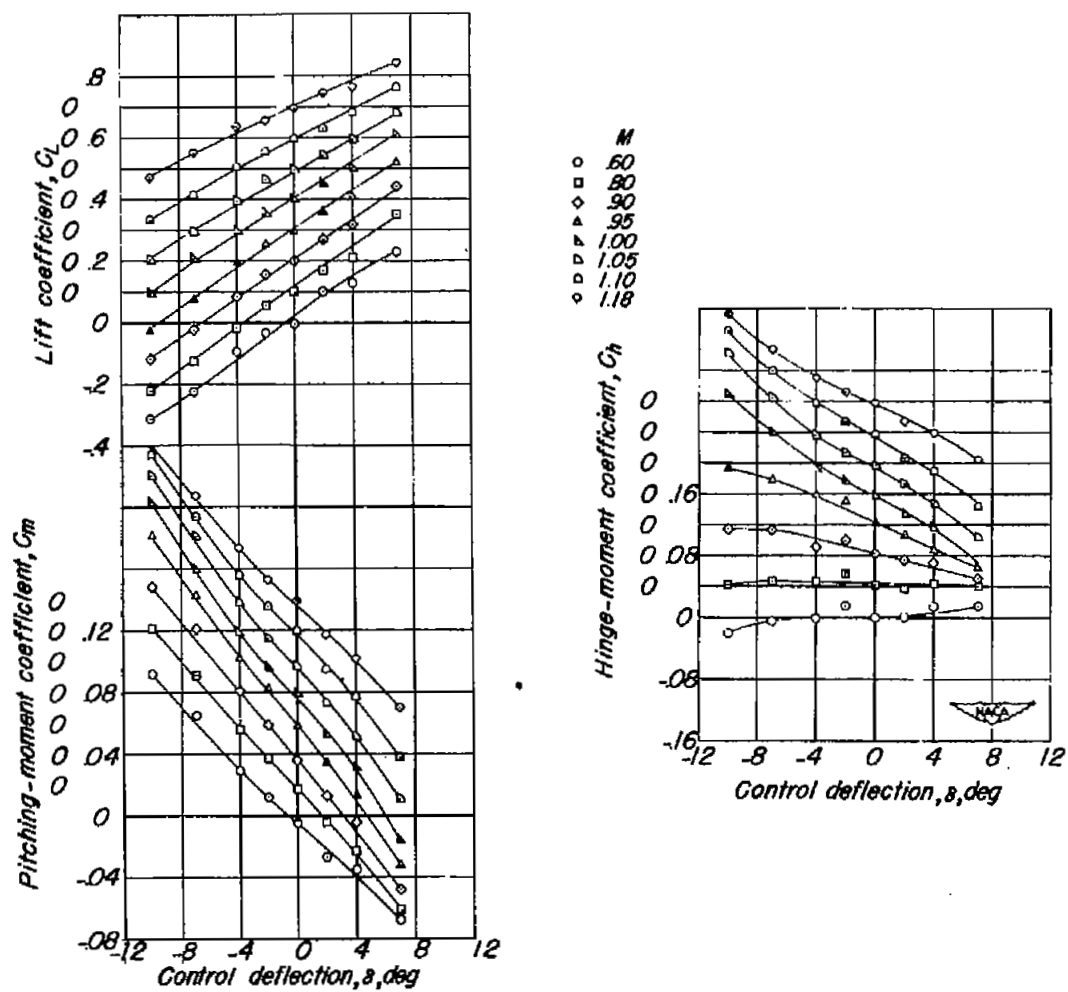


Figure 11, - Variation of aerodynamic characteristics with control deflection at various Mach numbers for a  $60^\circ$  delta wing having a  $0.20$ -constant-chord flap-type control with an unshielded triangular horn balance.  $\alpha = 0^\circ$ .

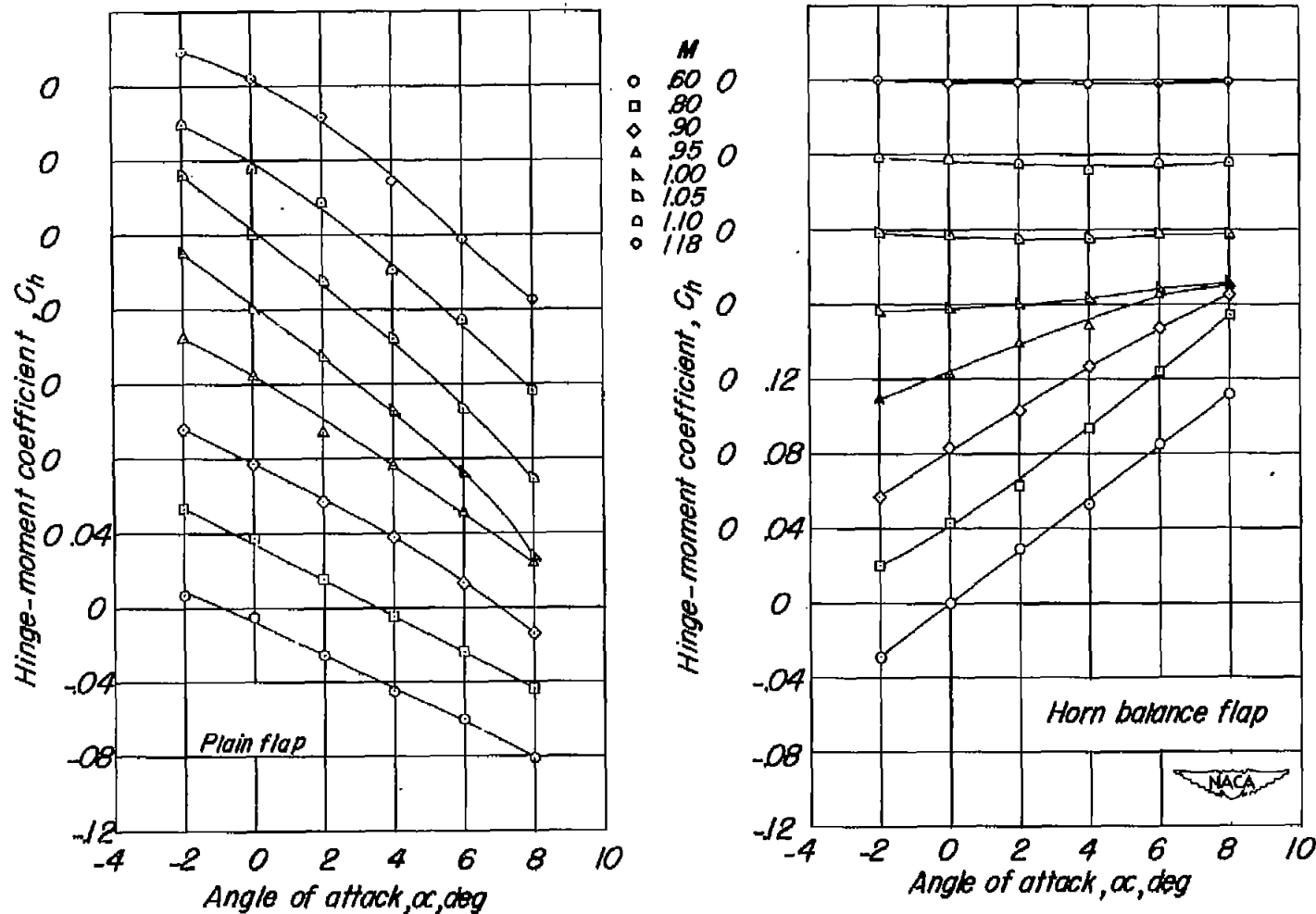


Figure 12.- Variation of hinge-moment coefficient with angle of attack at various Mach numbers for a  $60^\circ$  delta wing having a 0.20-constant-chord flap-type control with and without an unshielded triangular horn balance.  $\delta = 0^\circ$ .

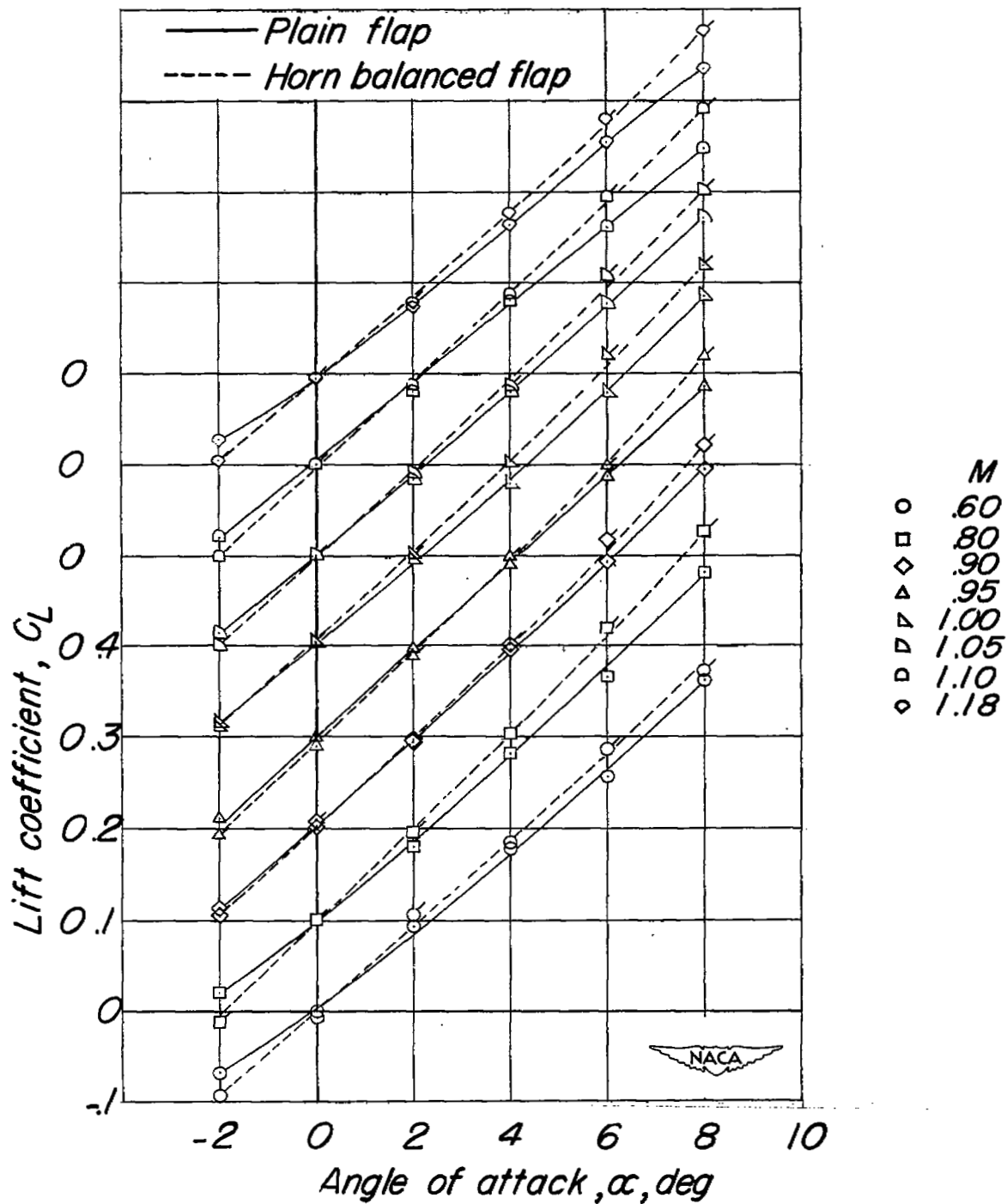


Figure 13.- Variation of lift coefficient with angle of attack for  $60^\circ$  delta wings at various Mach numbers.  $\delta = 0^\circ$ .

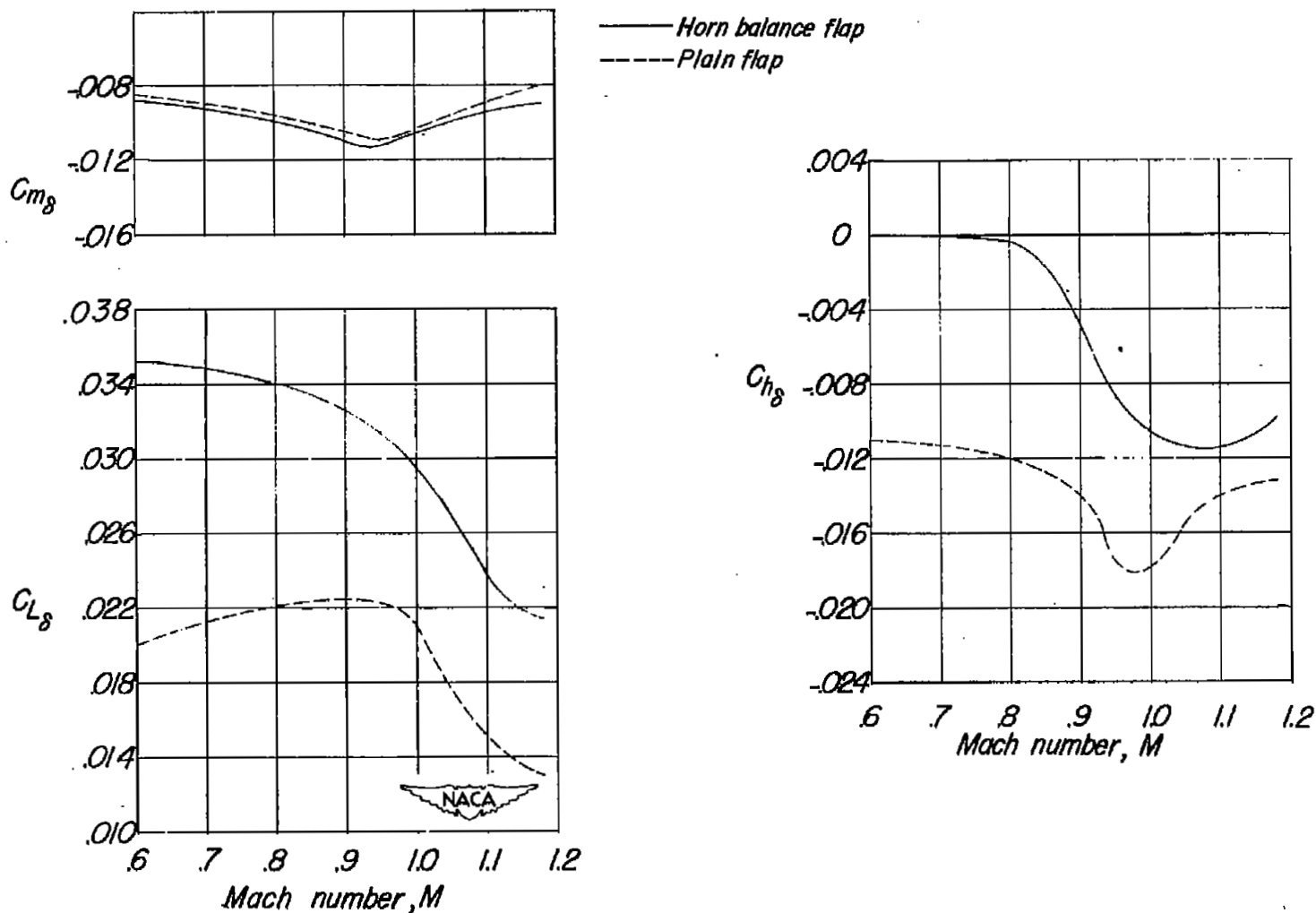


Figure 14.- Variation of control parameters,  $C_{L\delta}$ ,  $C_{m\delta}$ , and  $C_{h\delta}$  with Mach number for a  $60^\circ$  delta wing having a 0.20-constant-chord flap-type control with and without an unshielded triangular horn balance.

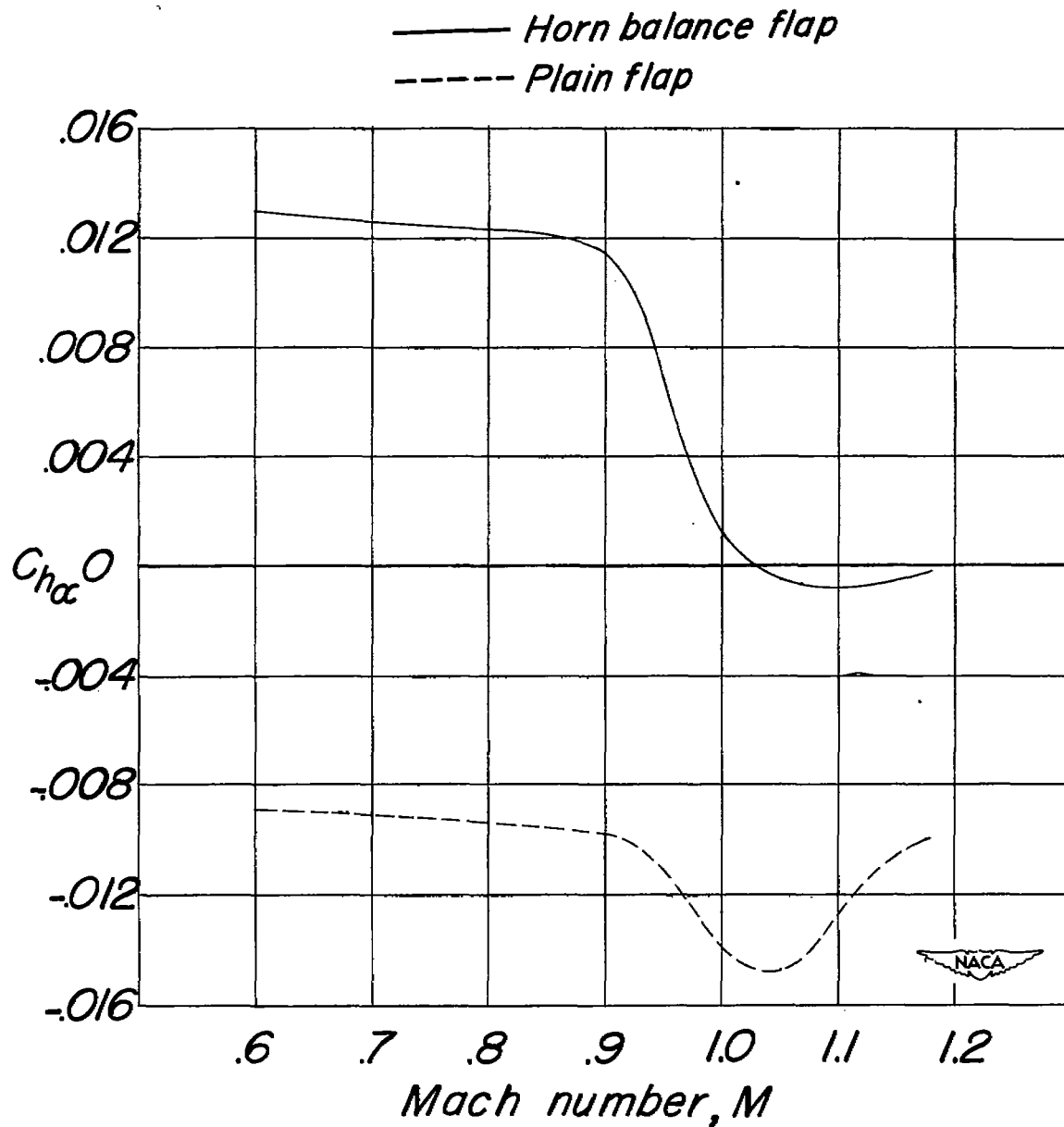
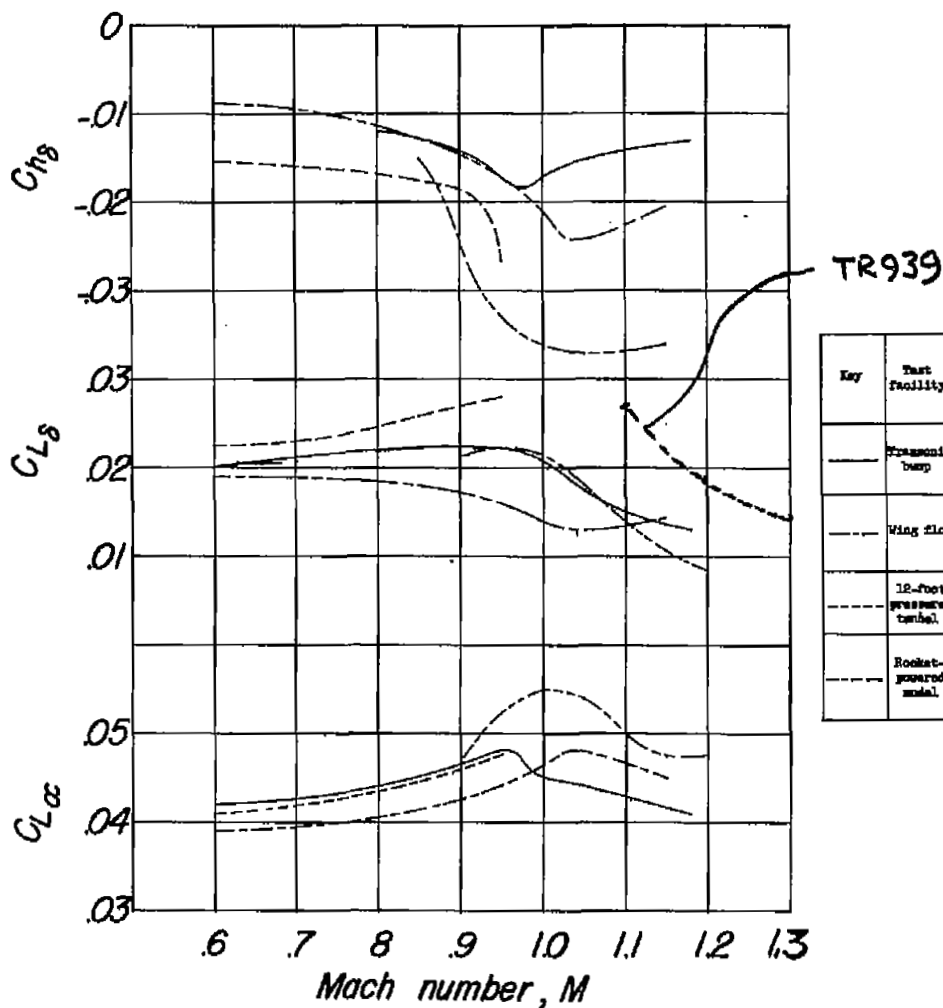


Figure 15.- Variation of control parameter  $C_{h\alpha}$  with Mach number for a  $60^\circ$  delta wing having a 0.20-constant-chord flap-type control with and without an unshielded triangular horn balance.  $\delta = 0^\circ$ .



Key	Test facility	Source of data	Leading edge sweepback (deg)	Aspect ratio	Airfoil section	Control chord, (percent root chord)	Reynolds number of tests	Remarks
—	Transonic bump	Present paper	60	2.31	NACA 65-006	20	1,300,000 to 1,400,000	Plain control
---	Wing flow	Reference 4	63.4	2.00	Double wedge	10.31	960,000 to 1,600,000	Plain control
----	12-foot pressure tunnel	Reference 5	63.03	2.00	Modified double wedge	10.75	5,300,000	Plain control
----	Rocket-powered model	Reference 6	60	2.31	NACA 65 <sub>06</sub> -006.5	12.5	10,000,000 to 20,000,000	Plain control with small triangular horn balance



Figure 16.- General comparison of lift effectiveness and hinge-moment parameter with Mach number for constant-chord flap-type controls of several models over a flap-angle range of  $-4^\circ$  to  $4^\circ$ .  $\alpha = 0^\circ$ .

SECURITY INFORMATION

NASA Technical Library



3 1176 01436 4492

